J|A|C|S
ARTICLES

Hydrogen-Bonding-Assisted Self-Doping in Tetrathiafulvalene (TTF) Conductor

Yuka Kobayashi,*,† Mayu Yoshioka,‡ Kazuhiko Saigo,‡ Daisuke Hashizume,§ and Takashi Ogura#

Waseda Institute for Advanced Study (WIAS), Waseda University, Tokyo, 169-8050, Japan, Department of Chemistry and Biotechnology, Graduate School of Engineering, The University of Tokyo, Tokyo 113-8656, Japan, Advanced Technology Support Division, RIKEN (The Institute of Physical and Chemical Research), Saitama 351-0198, Japan, and Consolidated Research Institute for Advanced Science and Medical Care (ASMeW), Waseda University, Tokyo 162-0041, Japan

Abstract: The synthesis, characterization, and carrier generation mechanism of self-doping in a tetrathiafulvalene (TTF) conductor, ammonium tetrathiafulvalene-2-carboxylate (TTFCOO$^-$NH$_4^+$), are described together with molecular orbital characteristics. Insulating TTFCOOH changes into a hole-doped conductor TTFCOO$^-$NH$_4^+$ with a conductivity of $\sigma = 2.0 \times 10^{-4}$ S/cm (300 K), upon salt formation with NH$_3$. A radical species, TTF$^{\bullet+}$COO$^-$NH$_4^+$, is generated via protonation of the TTF moiety as demonstrated by UV–vis, ESR, and ^{1}H NMR spectra. The X-ray crystallographic structure of TTFCOO$^-$NH$_4^+$ reveals supramolecular arrays of TTFCOO$^-$ moieties with short S···S contact, assisted by the one-dimensional hydrogen-bonding network composed of the ammonium and carboxylate ions. Molecular orbital calculations of cluster models show that the singly occupied molecular orbital (SOMO) of TTF$^{\bullet+}$COO$^-$NH$_4^+$ in the supramolecular array is not at the highest energy level, which is characterized as a quasi-closed-shell state. The *ab initio* periodic calculation with a one-dimensional boundary condition reveals that TTF$^{\bullet+}$COO$^-$NH$_4^+$ behaves as a dopant leading to the semiconducting behavior of the stacked TTF moieties assembled by the hydrogen-bonding network. Namely, TTFCOO$^-$NH$_4^+$ can be described as a "hydrogen-bonding-assisted self-doped conductor". The contribution of the hydrogen-bonding interaction to the electron conduction is experimentally supported by a large isotope effect in the ac conductivity of TTFCOO$^-$NH$_4^+$ at low temperature.

Introduction

Tetrathiafulvalene (TTF) chemistry has a long history since the first discovery of its conductivity in the 1970s.[1] Interests in the related molecules have spread into various fields concerned with electroactive materials because of their potential for the electronic devices such as field effect transistors (FETs),[2] and photovoltaic cells.[3] Carrier generation is the primary concern in order to obtain electroactive organic materials. The carriers in molecular conductors[4] are usually generated based on a charge-transfer mechanism between the electron donor and acceptor molecules, a mechanism that was proposed by Mulliken in the 1950s.[5] This mechanism is the underlying concept for carrier generation in the current molecular conductors, and thereafter has been extensively adopted for single-component molecular conductors.[6]

On the other hand, protonation of aromatic compounds by a Brønsted acid giving rise to radicals has been intensively studied since the 1990s.[7] This phenomenon also takes place with a typical donor molecule, TTF, because of the reactivity of the central carbon–carbon double bond toward a proton.[8] In 1994, Giffard et al. spectroscopically investigated the protonation of TTF with Brønsted acids in solution and found the generation

† Waseda Institute for Advanced Study (WIAS), Waseda University.
‡ The University of Tokyo.
§ RIKEN.
# Consolidated Research Institute for Advanced Science and Medical Care (ASMeW), Waseda University.

(1) (a) Wudl, F.; Wobschall, D.; Hufnagel, E. J. *J. Am. Chem. Soc.* **1972**, *94*, 670–672. (b) Ferraris, J.; Cowan, D. O.; Walatka, V. V.; Perlstein, J. H. *J. Am. Chem. Soc.* **1973**, *95*, 948–949.
(2) (a) Torrent, M. M.; Durkut, M.; Hadley, P.; Ribas, X.; Rovira, C. *J. Am. Chem. Soc.* **2004**, *126*, 984–985. (b) Bendikov, M.; Wudl, F.; Perepichka, D. F. *Chem. Rev.* **2004**, *104*, 4891–4945. (c) Rovira, C. *Chem. Rev.* **2004**, *104*, 5289–5317.
(3) (a) Hou, Y.; Chen, Y.; Liu, Q.; Yang, M.; Wan, X.; Yin, S.; Yu, A. *Macromolecules* **2008**, *41*, 3114–3119. (b) Berridge, R.; Skabara, P. J.; Pozo-Gonzalo, C.; Kanibolotsky, A.; Lohr, J.; McDouall, J. J. W.; McInnes, E. J. L.; Wolowska, J.; Winder, C.; Sariciftci, N. S.; Harrington, R. W.; Clegg, W. *J. Phys. Chem. B* **2006**, *110*, 3140–3152. (c) Kanato, H.; Narutaki, M.; Takimiya, K.; Otsubo, T.; Harima, Y. *Chem. Lett.* **2006**, *35*, 668–669.

(4) (a) Yamada, J.; Akutsu, H.; Nishikawa, H.; Kikuchi, K. *Chem. Rev.* **2004**, *104*, 5057–5083. (b) Geiser, U.; Schlueter, J. A. *Chem. Rev.* **2004**, *104*, 5203–5241. (c) Kato, R. *Chem. Rev.* **2004**, *104*, 5319–5346. (d) Shibaeva, R. P.; Yagubskii, E. B. *Chem. Rev.* **2004**, *104*, 5347–5378. (e) Fourmigué, M.; Batail, P. *Chem. Rev.* **2004**, *104*, 5379–5418. (f) Mori, H. *J. Phys. Soc. Jpn.* **2006**, *75*, 051003−15.
(5) Mulliken, R. S. *J. Am. Chem. Soc.* **1952**, *74*, 811–824.
(6) (a) Tanaka, H.; Okano, Y.; Kobayashi, H.; Suzuki, W.; Kobayashi, A. *Science* **2001**, *291*, 285. (b) Kobayashi, A.; Tanaka, H.; Kobayashi, H. *J. Mater. Chem.* **2001**, *11*, 2078. (c) Kobayashi, A.; Fujiwara, E.; Kobayashi, H. *Chem. Rev.* **2004**, *104*, 5243–5264.
(7) (a) Eberson, L.; Rander, F. *Acta Chem. Scand.* **1991**, *45*, 1093–1095. (b) Eberson, L.; Rander, F. *Acta Chem. Scand.* **1992**, *46*, 630–643. (c) Davies, A. G. *Chem. Soc. Rev.* **1993**, 299–304.

Scheme 1. The Radical Generation Mechanism Triggered by Protonation in TTF[8b]
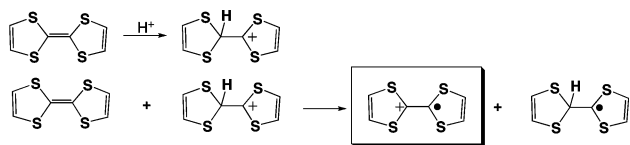
of a radical species, TTF[•+] from TTFH[+]. They proposed that TTF[•+] is generated via an electron transfer between protonated TTFH[+] and neutral TTF species,[8b] as shown in Scheme 1. Furthermore, they have also reported that TTF crystals treated with a Brønsted acid such as HBF₄, exhibit a small electronic conductivity of 10^{-10} S/cm, suggesting that TTF[•+] produced via the protonation of the TTF molecule could be the origin of the conductivity. However, neither the chemical properties of TTF[•+] nor its electronic state associated with the open-shell electron in the crystalline state is as yet well-understood,[8d] because of the lack of structural and molecular orbital information about this radical species in the crystal.

We have studied functional crystalline organic salts composed of ammonium and carboxylate ions, where formation of a one-dimensional hydrogen-bonding network plays a decisive role in determining their physical properties.[9] In the course of related research, we have serendipitously found that an ammonium salt of an acidic derivative of TTF, that is, ammonium tetrathiafulvalene-2-carboxylate (TTFCOO⁻NH₄⁺), exhibits conductivity. TTFCOO⁻NH₄⁺ is not a charge-transfer complex because NH₄⁺ has no electron-accepting property. Moreover, it is obvious that TTFCOO⁻NH₄⁺ is not an ion-radical salt because the stoichiometry of the ammonium and anionic TTF moieties are equivalent in this salt. Although the protonation-triggered radical generation of TTF originally proposed by Giffard et al. seems a possible mechanism in this phenomenon, no Brønsted acid was externally added to the salt. Carrier generation in such neutral closed-shell molecules is of particular interest and is worth investigating in detail because of its remarkable potential to produce unprecedented electroactive materials. In the present paper, we report the chemical, structural, and electronic properties of TTFCOO⁻NH₄⁺, together with molecular orbital characteristics, focusing on the role of the hydrogen-bonding interaction in the carrier generation.

Experimental Methods

General Methods. All reagents were purchased from Kanto Kagaku, Aldrich, Tokyo Chemical Industry, and Wako Pure Chemical. Diethyl ether was distilled from sodium/benzophenone ketyl[10] before use. ^{1}H NMR spectra were recorded on a Varian

Mercury 300 (300 MHz) and Bruker AVANCE system (600 MHz) instruments. FT-IR spectra were recorded on a Thermo Fisher SCIENTIFIC/Nicolet 6700. ESI-TOF-MS spectra were measured with a JEOL JMS-T100CS. The ESR spectrum was measured using crystalline powder with a JEOL JES-PX1060. Diffuse reflectance (UV−vis) spectra were recorded on a JASCO V-550. Powder X-ray diffraction data were collected with a Debye−Scherrer camera installed on the BL02B2 beamline at SPring-8 using 1.30380(7) Å radiations. The structure was solved and refined using the programs of DASH version 3.0[11] and RIETAN-FP,[12] respectively. Ac conductivities of pelletized polycrystalline samples were measured with a two-probe method at 1 MHz from 4.2 to 320 K with an LCR meter (Agilent 4284 A) in a liquid He cryostat.

Preparation of Materials. TTFCOO⁻NH₄⁺. Tetrathiafulvalene-2-carboxylic acid, TTFCOOH was synthesized from TTF in two steps, following the reported procedure.[13] TTFCOOH (205 mg, 0.825 mmol) was dissolved in Et₂O (40 mL) and the resulting solution was filtered off from a trace amount of insoluble fractions (this process is unnecessary for the freshly prepared TTFCOOH). A small portion of 28% aqueous solution of ammonia (50 µL) was added to the filtrate and the resulting mixture was stirred for 15 s under ultrasonication to afford precipitates (ultrasonication increases yields of TTFCOO⁻NH₄⁺). The polycrystalline solids were collected by filtration, washed with Et₂O (20 mL), and then dried in vacuo to afford pure TTFCOO⁻NH₄⁺ (109 mg, 0.411 mmol, 50%) as a dark orange solid. Anal. Calcd for C₇H₇NO₂S₄ (265.40): C, 31.68; H, 2.66; N, 5.28. Found. C, 31.59; H, 2.75; N, 5.10. IR (KBr; cm⁻¹): 3053.5, 3329.2, 2777.8, 1547.8, 1537.0, 1364.9, 1046,6, 737.9. ^{1}H NMR (DMSO-d_6; ppm): δ = 7.67 (s, 1H), 6.75 (s, 2H). Use of saturated methanolic solution of ammonia instead of 28% aqueous solution also affords conductive TTFCOO⁻NH₄⁺.

TTFCOO⁻ND₄⁺. Tetrathiafulvalene 2-carboxylic acid (TTFCOOH) (225 mg, 0.906 mmol) was dissolved in CH₃OD (30 mL), and the resulting solution was filtered from the insoluble fractions. The filtrate was evaporated to dryness under reduced pressure. This operation was repeated four times to afford deuterated TTFCOOD. TTFCOOD (105 mg, 0.421 mmol) was dissolved into dry Et₂O (25 mL), and the resulting solution was filtered from the insoluble fractions. A small portion of a D₂O solution of ND₃ (26%, 65 µL) was added to the resulting solution, and the resulting mixture was stirred for 15 s under ultrasonication to afford a crystalline precipitate. The polycrystalline solids were collected by filtration, and then washed with dry Et₂O (2 mL × 3) and deuterated toluene (1 mL). The collected crystals were dried in vacuo to afford pure TTFCOO⁻ND₄⁺ (79.4 mg, 0.294 mmol, 33%) as a dark orange solid. ESI-TOF-MS spectrometry indicates quantitative substitution of the ammonium protons of TTFCOO⁻ND₄⁺ with deuterons (see Supporting Information (SI), Figure S1). Anal. Calcd for C₇H₃D₄NO₂S₄ (269.42): C, 31.21; H, 2.62; N, 5.20. Found. C, 3.14; H, 2.50; N, 5.17. IR (KBr; cm⁻¹): 3053.5, 2777.8, 1548.2, 1537.7, 1366.4, 1046,6, 738.1. ^{1}H NMR (DMSO-d_6; ppm): δ = 7.67 (s, 1H), 6.75 (s, 2H).

Theoretical Methods. The geometry was fully optimized with unrestricted density functional theory employing Becke's three-parameter exchange and Lee−Yang−Parr's correlation functionals,[14] UB3LYP/6-31G*, and the single point energy was evaluated with unrestricted Møller−Plesset second-order perturbation theory,[15] UMP2/6-31G* for the potential energy surface (PES) of the carrier generation. Orbital energies and coefficients for a tetrameric model were determined with UHF/6-31G* and UMP2/3-21G*. The configuration interaction was evaluated with complete-

(8) (a) Cavara, L.; Gerson, F.; Cowan, D. O.; Lerstrup, K. *Helv. Chim. Acta* **1986**, *69*, 141–151. (b) Giffard, M.; Alonso, P.; Garin, J.; Gorgues, A.; Nguyen, T. P.; Richomme, P.; Robert, A.; Roncali, J.; Uriel, S. *Adv. Mater.* **1994**, *6*, 298–300. (c) Giffard, M.; Gorgues, A.; Riou, A.; Roncali, J.; Alonso, P.; Uriel, S.; Grin, J.; Nguyen, T. P. *Syn. Met.* **1995**, *70*, 1133–1134. (d) Giffard, M.; Sigalov, M.; Khodorkovsky, V.; Gorgues, A.; Mabon, G. *Syn. Met.* **1999**, *102*, 1713.

(9) (a) Kobayashi, Y.; Kodama, K.; Saigo, K. *Org. Lett.* **2004**, *6*, 2941–2944. (b) Kobayashi, Y.; Kurasawa, T.; Saigo, K. *J. Org. Chem.* **2004**, *69*, 7436–7441. (c) Kobayashi, Y.; Saigo, K. *J. Am. Chem. Soc.* **2005**, *127*, 15054–15060. (d) Kodama, K.; Kobayashi, Y.; Saigo, K. *Chem.−Eur. J.* **2007**, *13*, 2144–2152. (e) Kodama, K.; Kobayashi, Y.; Saigo, K. *Cryst. Growth Des.* **2007**, *7*, 935–939. (f) Kobayashi, Y.; Soetrisno; Kodama, K.; Saigo, K. *Tetrahedron: Asymmetry* **2008**, *19*, 295–301.

(10) The sodium/benzophenone ketyl can both react with air and moisture, and act as an indicator. The hazard of such refluxing solutions is if the flask is exposed to air, in which the alkali metal can ignite the hydrocarbon solvent, causing a fire.

(11) David, W. I. F.; Shankland, K.; Streek, K.; Pidcock, E.; Motherwell, W. D. S.; Cole, J. C. *J. Appl. Crystallogr.* **2006**, *39*, 910–915.

(12) RIETAN-FP: A multi-purpose pattern-fitting system. Izumi, F.; Ikeda, T. *Mater. Sci. Forum* **2000**, *321−324*, 198−203.

(13) Garín, J.; Orduna, J.; Uriel, S.; Moore, A. J.; Bryce, M. R.; Wegener, S.; Yufit, D. S.; Howard, J. A. K. *Synthesis* **1994**, *5*, 489–494.

(14) (a) Becke, A. D. *J. Chem. Phys.* **1993**, *98*, 5648–5652. (b) Lee, S.; Yang, W.; Parr, R. G. *Phys. Rev. B* **1988**, *37*, 785–786.

(15) Møller, C.; Plesset, M. S. *Phys. Rev.* **1934**, *46*, 618–622.
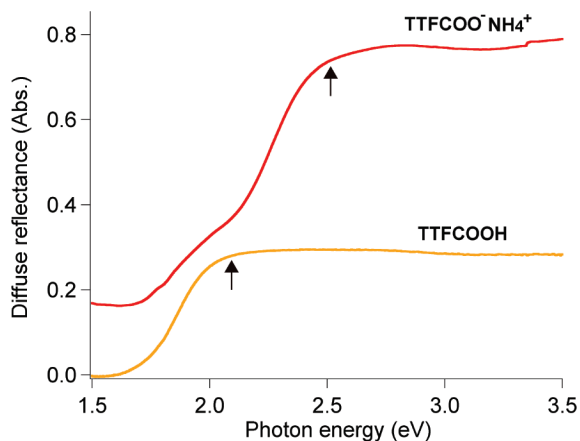
Figure 1. Diffuse reflectance spectra of TTFCOOH (yellow) and TTFCOO$^-$NH$_4^+$ (red). Arrows indicate the edges of the absorption corresponding to the excitation of intraband.

Scheme 2. Preparation of TTFCOO$^-$NH$_4^+$
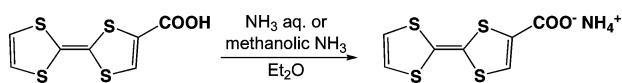
active-space self-consistent field (CASSCF)[16] applying seven electrons distributed among eight orbitals (7, 8) as an active space using 3-21G*. The active space was selected to include the SOMO and the orbitals with similar characteristics to the SOMO. The *ab initio* periodic calculation was carried out taking into account one-dimensional periodicity along *b**-axis with a cutoff value of 100 Bohr. Brillouin zone sampling was done using $1 \times 40k \times 1$ points. All calculations were performed using the Gaussian 03 program package[17] on a workstation constructed with 8-way/16-core AMD OpteronD (Visual Technology Co. Ltd.).

Results and Discussion

Radical Generation in TTFCOO$^-$NH$_4^+$. TTFCOO$^-$NH$_4^+$ was prepared from TTFCOOH and aqueous NH$_3$ or methanolic ammonia as a fine crystalline powder as shown in Scheme 2. IR spectroscopy of TTFCOO$^-$NH$_4^+$ showed the disappearance of the absorption band at 1660 cm^{-1} corresponding to the C=O stretching vibration of TTFCOOH,[18] and the appearance of a peak at 1547 cm^{-1} corresponding to the carboxylate stretching vibration (see SI, Figure S2), indicating the salt formation, $-$COO$^-$ and NH$_4^+$ in the crystal. This means that the dominant intermolecular interaction between TTFCOO$^-$ and NH$_4^+$ is not a nonionic hydrogen bonding but a stronger electrostatic hydrogen-bonding interaction.[19] The color of the obtained crystalline powder was dark orange, which is neither typical of an ion-radical salt nor a charge-transfer salt.

While TTFCOOH is an insulator, TTFCOO$^-$NH$_4^+$ exhibits a value for the ac conductivity of 2.0×10^{-4} S/cm at 300 K using a two-probe method. Diffuse reflectance (UV$-$vis) spectra of TTFCOOH and TTFCOO$^-$NH$_4^+$ are shown in Figure 1. The absorbance of TTFCOO$^-$NH$_4^+$ in the low photon energy region is assignable as an intraband excitation corresponding to the plasma oscillation of the mobile carriers. The edge of the

absorbance of insulating TTFCOOH is shifted to the higher energy region by 0.4 eV upon salt formation, as indicated with the arrows, which corresponds to the Fermi energy of holes generated in the valence band. These UV$-$vis spectra clearly show a drastic change in the electronic state from an insulator, TTFCOOH, to a conductor, TTFCOO$^-$NH$_4^+$. A similar shift of the excitation energy is also observed in the protic doping process of π-conjugated polymers.[20]

ESR spectrum of crystalline TTFCOO$^-$NH$_4^+$, measured at 103 K, showed the signal of radical species (see SI, Figure S3). The *g*-value of the radical is 2.0069, which is very close to that of TTF$^{\bullet+}$ in typical organic metals composed of TTF derivatives.[8a,21] These results strongly suggest generation of the radical species TTF$^{\bullet+}$COO$^-$NH$_4^+$ in TTFCOO$^-$NH$_4^+$ crystals. Assuming that the detected radical is localized, comparison of the peak area of the signal with that of a standard organic free radical molecule, 1,1-diphenyl-2-picrylhydrazyl, suggests that one spin exists per 6.2 TTFCOO$^-$NH$_4^+$ units (16%) at 300 K.

UV$-$vis and ESR spectra clearly show that TTFCOOH gives rise to a charge carrier upon salt formation. In this process, no external addition of Brønsted acid is necessary to generate conductivity in TTFCOO$^-$NH$_4^+$, meaning that TTFCOO$^-$NH$_4^+$ can be characterized as a self-doped conductor.

Mechanism of Radical Generation in TTFCOO$^-$NH$_4^+$ Crystals. A plausible mechanism of radical generation in TTFCOO$^-$NH$_4^+$ crystals is shown in Scheme 3. This mechanism essentially follows that for the protonation-triggered spin generation of TTF proposed by Giffard et al.[8b] (Scheme 1). It is known that the protonation of TTF occurs at the central carbon$-$carbon double bond rather than the electron-rich sulfur atoms due to thermodynamical stability of TTFH$^+$, as demonstrated by X-ray crystallographic analysis.[8c,22] The potential energy surface (PES) for the protonation of TTF (Figure 2, black) suggested that the formation energy of the protonated species, TTFH$^+$, is quite large, $-$231.4 kcal/mol, which is consistent with the experimental facts. The energy required for the electron-transfer reaction from the neutral donor (TTF) to TTFH$^+$ to generate radical species (TTFH$^{\bullet}$ + TTF$^{\bullet+}$) is 20.4 kcal/mol. The PES for the protonation of TTFCOO$^-$NH$_4^+$ (Figure 2, blue) also suggested that the formation energy of TTFH$^+$COO$^-$NH$_4^+$ and subsequently occurring radical generation by electron transfer from TTFH$^+$COO$^-$NH$_4^+$ are $-$252.5 and 18.2 kcal/mol, respectively. These theoretical calculations in the gas phase indicate that the self-protonation followed by radical generation of TTFH$^+$COO$^-$NH$_4^+$ shown in Scheme 3 is energetically similar to that for TTF and therefore is possible.

Both NH$_4^+$ and TTFCOOH are possible proton donors in this system (Scheme 3). In fact, ^{1}H NMR spectroscopy of TTFCOOH in CD$_3$CN showed a small singlet signal at 6.93 ppm corresponding to the proton attached on the sp^3 carbon of the protonated TTF moiety, suggesting partial self-protonation in CD$_3$CN (see SI, Figure S4a). Furthermore, the filtrate in CD$_3$CN obtained by separation of the precipitated crystals of TTFH$^+$COO$^-$NH$_4^+$ showed a set of singlet signals at $\delta = 6.45$, 6.77, and 8.36 ppm (see SI, Figure S4b) with an intensity ratio

(16) Roos, B. O. In *Advances in Chemical Physics; Ab Initio Methods in Quantum Chemistry - II*; Lawley, K. P., Ed.; John Wiley & Sons Ltd.: Chichester, England, 1987; p 399.

(17) Frisch, M. J. et al.; *Gaussian 03, Revision D. 02*; Gaussian, Inc.: Wallingford, CT, 2004.

(18) Green, D. C. *J. Org. Chem.* **1979**, *44*, 1476–1479.

(19) (a) Desiraju, G. R. *Acc. Chem. Res.* **2002**, *35*, 565–573. (b) Alavi, S.; Thompson, D. L. *J. Chem. Phys.* **2003**, *118*, 2599–2605.

(20) (a) Chaudhuri, D.; Kumar, A.; Rudra, I.; Sarma, D. D. *Adv. Mater.* **2001**, *13*, 1548–1551. (b) Lebedev, M. Y.; Lauritzen, M. V.; Curzon, A. E.; Holdcroft, S. *Chem. Mater.* **1998**, *10*, 156–163.

(21) (a) Tomkiewicz, Y.; Taranko, A. R.; Torrance, J. B. *Phys. Rev. B.* **1980**, *22*, 3113–3118. (b) Khodorkovsky, V.; Shapiro, L.; Krief, P.; Shames, A.; Mabon, G.; Gorgues, A.; Giffard, M. *Chem. Commun.* **2001**, 2736–2737.

(22) Giffard, M.; Frère, P.; Gorhues, A.; Riou, A.; Roncali, J.; Toupet, L. *J. Chem. Soc. Chem. Commun.* **1993**, 944–945.

Scheme 3. A Plausible Mechanism of Radical Generation in TTFCOO⁻NH₄⁺ Crystals[a]

a)

b)

c)
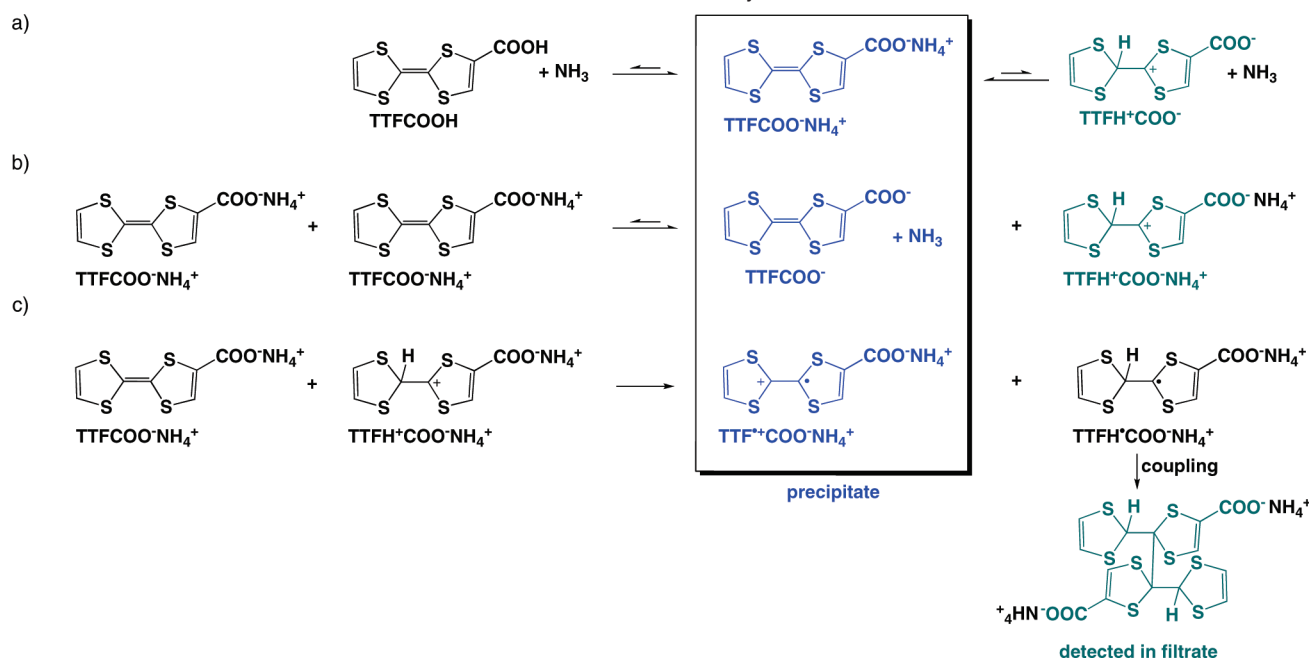
[a] (a and b) Self-protonation of TTFCOO⁻NH₄⁺ in the acid–base equilibrium. (c) Electron-transfer reaction between TTFCOO⁻NH₄⁺and TTFH⁺COO⁻NH₄⁺. The chemical species represented by light blue were detected by ¹H NMR and ESI-TOF-MS analyses.
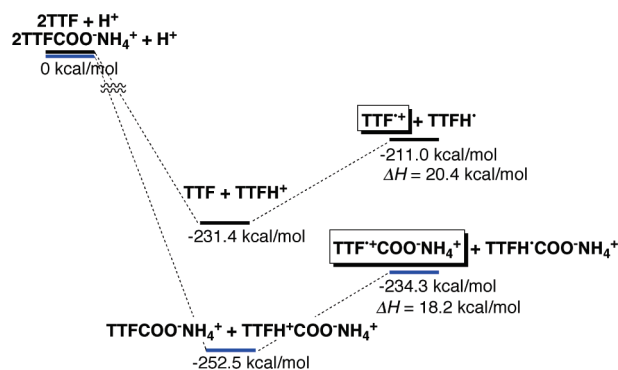
Figure 2. PES of the protonation and electron-transfer processes of TTFCOO⁻NH₄⁺ (blue) and TTF (black). The geometries were fully optimized with UB3LYP/6-31G*, and the single point calculations were carried out with UMP2/6-31G* using the optimized geometries. ΔH corresponds to the formation enthalpy of the radical species.

of 2:1:1, which are consistent with the reported chemical shifts of the protons of TTFH⁺.[8b] According to these spectral observations, it is strongly suggested that the formation of TTFH⁺COO⁻NH₄⁺ takes place during the crystallization process of TTFCOO⁻NH₄⁺ (Scheme 3b). It should be noted here that the self-protonation of TTFCOO⁻NH₄⁺ shown in Scheme 3b is accompanied by the formation of TTFCOO⁻ and NH₃, which would be indistinguishable from those resulting from the above-mentioned equilibrium (Scheme 3a, left) between ionic TTFCOO⁻NH₄⁺ and nonionic TTFCOOH + NH₃ in the crystal. TTFCOO⁻, generated by the self-protonation in Scheme 3b, would formally play a role as a counteranion of the positive charge of TTF·⁺COO⁻NH₄⁺ to keep the total charge of the crystals to be neutral.

¹H NMR spectroscopy also suggested that a filtrate contains the second species in addition to TTFH⁺COO⁻NH₄⁺, which displays a set of singlet signals at δ = 3.49, 6.42, and 6.93 ppm with an intensity ratio of 1:2:1. The signal at 3.49 ppm is assignable as a methine proton of (TTFHCOO⁻NH₄⁺)₂ probably

being derived from coupling of the unstable radical species, TTFH·COO⁻NH₄⁺ (Scheme 3c). Moreover, ESI-TOF-MS spectrometry of the filtrate in CH₃CN treated with trime-thylsilyldiazomethane showed a signal corresponding to (TTFHCOOMe)₂ [calcd. for C₁₈H₁₇NO₄S₈ (C₁₆H₁₄O₄S₈ + CH₃CN), m/z: 566.89232; found, m/z: 566.89065 (−1.67 mmu) (see SI, Figure S4c)], strongly supporting the generation of (TTFHCOO⁻NH₄⁺)₂.

Here, it should be noted that TTFCOOH crystal is an insulator. Nevertheless, the ¹H NMR spectrum of TTFCOOH in CD₃CN (see SI, Figure S4a) suggests a trace amount of TTFH⁺COOH and (TTFHCOOH)₂, probably formed from the self-protonation followed by the electron-transfer reactions. This indicates that the generation of radical species in solution does not directly lead to the stabilization of radicals and achievement of the conductivity in the crystal. Obviously, the salt formation of TTFCOOH with NH₃ is the key in the generation of the carriers and realization of the conductivity in TTFCOO⁻NH₄⁺ crystals.

Crystal Structure of TTFCOO⁻NH₄⁺ Determined by Powder X-ray Diffraction. The radical species, TTF·⁺COO⁻NH₄⁺, is detected only in the solid state, which implies that carrier generation is strongly correlated with the molecular arrangement in the crystal. The crystal structure of TTFCOO⁻NH₄⁺ was determined by the Rietveld method[10,11] from the powder X-ray diffraction data collected at 300 K using synchrotron radiation (see SI, Figure S5 and Figure 8).[23] As shown in Figure 3a, a one-dimensional columnar hydrogen-bonding network is formed by TTFCOO⁻ ions and NH₄⁺, where TTFCOO⁻ ions are stacked along the b-axis with intermolecular S···S and π/π interactions. The neighboring columns along the c-axis are connected together by hydrogen bonds via ammonium ions forming a two-dimensional sheet (Figure 3b), allowing interactions of TTF-

_____

(23) C₇H₇NO₂S₄, *Monoclinic*, P2₁, a = 6.245 (3) Å, b = 8.43 (1) Å, c = 20.30 (1) Å, β = 90.82 (3) deg, V = 1068.6 (1) (Å³), Z = 4, R = 0.080.
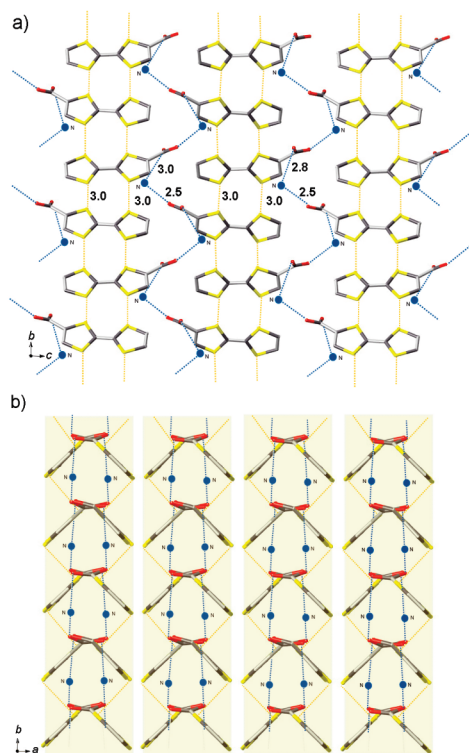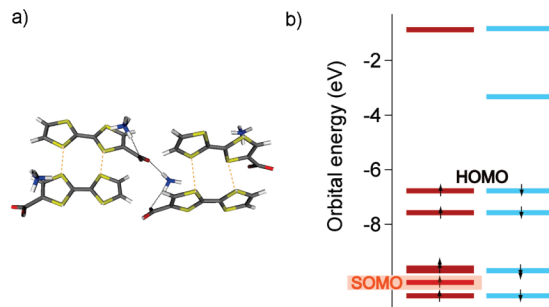
Figure 3. Crystal structure of TTFCOO$^-$NH$_4^+$. (a) Side view of one-dimensional (1D) hydrogen-bonding (HB) network. (b) The supramolecular sheets with hydrogen-bonding network and S···S contacts parallel to the *ab*-plane. Blue and yellow dotted lines show hydrogen-bonding interaction and S···S contacts, respectively. Hydrogen-bonding interaction was assigned by the distance between N and O atoms. Hydrogen atoms are omitted for clarity.

COO$^-$ ions in two dimensions through hydrogen bonds, π/π interaction, and S···S interactions. The S···S distance is 3.0 Å, and it is 0.7 Å shorter than the sum of the van der Waals radii. This remarkably short contact between TTF moieties is likely to be achieved by the predominant electrostatic hydrogen-bonding interaction between TTFCOO$^-$ and NH$_4^+$ moieties. The one-dimensional TTFCOO$^-$ column connected with the effective S···S contact offers a possible conduction pathway.

The control of molecular arrays utilizing weak interactions such as hydrogen bonds, π/π interaction, and S···S contact, aiming to increase the dimensionality of interactions between components in the crystal, is a current trend in the design of charge-transfer conductors.[24,4e] The crystal structure of TTFCOO$^-$NH$_4^+$ determined here represents a new strategy for achieving two-dimensional intermolecular interaction of TTF derivatives in the crystal, which makes use of the electrostatic hydrogen-bonding network composed of ammonium and carboxylate ions.[9]

Electronic State of the Doped Supramolecular Assembly of TTFCOO$^-$NH$_4^+$. Because the importance of the assembly of molecules in the crystal in self-doping of TTFCOO$^-$NH$_4^+$ was strongly suggested by the experimental results, we investigated the electronic state of the radicals in the supramolecular array by theoretical calculations. A tetrameric assembly of

(24) (a) Bryce, M. R. *J. Mater. Chem.* **1995**, *5*, 1481–1496. (b) Baudron, S. A.; Avarvari, N.; Batail, P.; Coulon, C.; Clérac, R.; Canadell, E.; Auban-Senzier, P. *J. Am. Chem. Soc.* **2003**, *125*, 11583–11590. (c) Murata, T.; Morita, Y.; Fukui, K.; Sato, Shiomi, D.; Takui, T.; Maesato, M.; Yamochi, H.; Saito, G.; Nakasuji, K. *Angew. Chem., Int. Ed.* **2004**, *43*, 6343–6346.

Figure 4. Electronic state of the supramolecular assembly of TTFCOO$^-$NH$_4^+$, evaluated with UHF/6-31G*. (a) Tetrameric model. Black and yellow dotted lines represent hydrogen bonds and S···S contacts, respectively. (b) Molecular orbital energies in electronvolts (eV) and electron configurations. Red and light blue bars represent alpha- and beta-orbitals, respectively. Arrows mean up/down-spins.
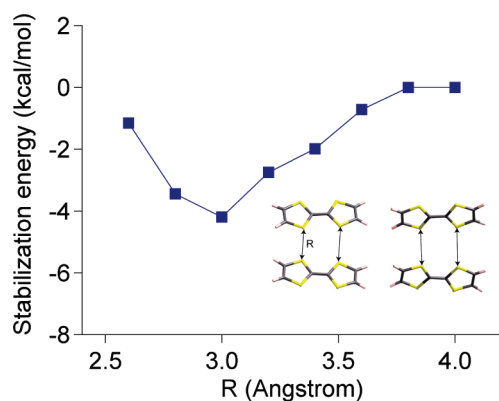
TTFCOO$^-$NH$_4^+$ was extracted from the X-ray structure as a minimal supramolecular model in the crystal, where all molecules interact with each other via hydrogen-bonding interaction or short S···S contact (Figure 4a). C1 symmetry was adopted in the calculation of the tetramer. The single point calculations were carried out with UHF/6-31G* for the tetrameric unit of TTFCOO$^-$NH$_4^+$, assuming one radical cation in each model ($S = 1/2$, charge $= +1$). The calculated molecular orbital energies of the unit near the frontier orbitals are shown in Figure 4b. Surprisingly, the energy level of the SOMO of the tetrameric assembly is not at the highest occupied level but at the fifth level from the highest occupied molecular orbital (HOMO). In sharp contrast, the SOMO of monomeric TTFCOO$^-$NH$_4^+$ lies at the highest occupied energy level (see SI, Figure S6). Namely, the open-shell electron of TTF$^{\bullet+}$COO$^-$NH$_4^+$ embedded in the closed-shell TTFCOO$^-$NH$_4^+$ molecules does not occupy the frontier orbital; it behaves as if it is in a closed-shell molecule (quasi-closed-shell state[25]).

Such a quasi-closed-shell state in a molecular conductor is anomalous. Restricted open-shell Hartree–Fock (ROHF) promising the highest SOMO gives the total energy as 3.2 kcal/mol higher than that evaluated with UHF/6-31G*. Although spin contamination is quite small in the UHF calculation, with a value of 0.7523 for $\langle S^2 \rangle$, the reliability of the UHF calculation should be confirmed by more accurate calculations taking into account the electron-correlation effect, because configuration interaction (CI) is critical for representation of complicated open-shell systems.[26] Hence, a multireference treatment was adopted for the single point calculation of the tetrameric assembly with CASSCF using 3-21G*, which revealed that the contribution of the main configuration to the wave function is 91% (see SI, Figure S7). The singly occupied molecular orbitals in the CASSCF configurations are mostly identical with the lowered SOMO in the UHF calculation, which means that the radical is stable without the effect of CI. On the other hand, the dynamical correlation effect[26] hardly contributes to the orbital energies from a calculation with UMP2 (see SI, Figure S8), as expected. Furthermore, other basis sets or a hexameric model also reproduce this particular electronic state (see SI, Figure S9). Therefore, the UHF calculations using the cluster models are essentially reliable representing the present open-shell system.

(25) Löwdin, P. O.; Brändas, E.; Kryachko, E. S. In *Fundamental World of Quantum Chemistry: A Tribute to the Memory of Per-Olov Löwdin*; Springer: Berlin, 2003; p 380.
(26) Kobayashi, Y.; Kamiya, M.; Hirao, K. *Chem. Phys. Lett.* **2000**, *319*, 695–700.

Figure 5. The dependence of the stabilization energy of SOMO of TTF_4 on the S···S distance, evaluated with UHF/6-31G*. The relative energy difference of SOMO compared with the value at 4.0 Å is plotted in kcal/mol.

It is worth noting that quasi-closed-shell configurations have been observed in inorganic compounds including transition metal elements with d electrons, or lanthanide or actinide elements with f electrons, and have attracted considerable experimental[27] and theoretical interests.[28] However, it is quite a rare phenomenon in organic or organometallic molecules; very recently, 2,2,6,6-tetramethylpiperidine-1-oxy radical (TEMPO) derivatives covalently connected with a delocalized aromatic skeleton[29a] or a Pt complex unit[29b] have been reported to show this particular electronic state. To the best of our knowledge, $TTFCOO^-NH_4^+$ is the first conductor in "f-electron-like system" composed of purely organic elements.

Effect of Short S···S Contact in the Stabilization of the SOMO. What is the key factor for stabilizing the SOMO in the supramolecular array? As described above, the X-ray crystallographic analysis of $TTFCOO^-NH_4^+$ showed unusually short S···S contacts between the TTF moieties. To focus on the role of these short S···S contacts in the stabilization of the SOMO, molecular orbitals of a new tetrameric model composed of TTF molecules (TTF_4) without hydrogen-bonding functionalities were calculated using UHF/6-31G*.[30] As a result, the quasi-closed-shell state is also appeared in TTF_4 (see SI, Figure S10). The dependence of the stabilization of the SOMO on the S···S distance was investigated as follows. The S···S distance (R) in TTF_4 was changed in incremental steps of 0.2 Å from 2.6 to 4.0 Å, where the energy of the SOMO at each step was evaluated with UHF/6-31G*. Figure 5 shows the relative energy of the SOMO of TTF_4 at various S···S distances compared with the energy at 4.0 Å. The experimentally observed S···S

contact, 3.0 Å, gives the minimum energy of −4.2 kcal/mol in this plot. Therefore, the short S···S contacts are suggested to be very important in the stabilization of the SOMO. It is noteworthy that the optimal S···S distance between $TTF^{•+}$ radical species in a dimeric model of $(TTF)_2$-$(ClO_4)_2$, optimized with MCQDPT/CASSCF(2,2), is reported to be 3.24 Å by Noboa, et al.,[31] and it is closely related to the present system. The hydrogen-bonding part seems dispensable for achieving the quasi-closed-shell configuration. However, it should play a role in achieving such short S···S contacts, even with Coulomb repulsion between TTF moieties.

Role of the Embedded Radicals in Conductive $TTFCOO^-$-NH_4^+. To obtain a deeper insight into the role of $TTF^{•+}$-$COO^-NH_4^+$ in conductive $TTFCOO^-NH_4^+$, the periodic calculation taking into account the one-dimensional periodicity of the crystal along one of reciprocal lattice vectors, b^*-axis, was investigated, where two TTF columns connected by the hydrogen-bonding network are assumed as the replication direction. Actually, in this calculation, the tetrameric cluster shown in Figure 4a was adopted as a primitive unit where one $TTFCOO^-NH_4^+$ unit in the tetrameric model was replaced by ($TTFCOO^-$ + NH_3), which is likely produced during the self-protonation process shown in Scheme 3b. This species helps to neutralize the total charge of the crystal. The electronic states of the hydrogen-bonding ammonium salt crystals are well-represented by *ab initio* all-electron periodic Hartree−Fock (HF) method.[9c] Moreover, the periodic unrestricted HF approach has been applied to some transition metal compounds, and exhibited the superior performances in representing their magnetic properties as well as crystal structures.[32] Therefore, the calculation was carried out with periodic UHF method. Here, Gaussian code[17] was used to compare the result with that of the cluster model. Actually, the modified tetrameric model as mentioned above was evaluated with periodic-boundary-condition (PBC)-UHF/3-21G*, assuming a doublet with neutral charge ($S = 1/2$, charge = 0). As shown in Figure 6a, SOMO in the quasi-closed-shell configuration also resulted in this modified neutral tetrameric cluster of $TTFCOO^-NH_4^+$ (nonPBC). The molecular orbital of SOMO (Figure 6c, a1) is significantly localized, differently from the orbitals of a typical proton-doped conductor, polyaniline, which delocalize over the conjugated π-orbitals.[33] The SOMO induces lowered LUMO, which possesses a similar orbital character with the SOMO in relation of antisymmetry (Figure 6c, a2).[34] In the PBC calculation, the lowered LUMO (PBC-LUMO) (Figure 6b, b2) shows strong energy dispersion along the b^* lattice vector, lying 0.3 eV higher than the highest occupied energy level at M point ($k = b^*/2$). The energy level of PBC-LUMO caused by PBC-SOMO possibly acts like an acceptor level in the band gap in classical inorganic p-type semiconductors,[35] which is supported by the spectroscopic observation shown in Figure 1. It is of interest that the alpha- and beta-orbitals right above PBC-SOMO are largely split, where the beta-orbital (Figure 6b, b3) is suggested to correlate

(27) (a) Ohta, H.; Nomura, K.; Hiramatsu, H.; Ueda, K.; Kamiya, T.; Hirano, M.; Hosono, H. *Solid-State Electron.* **2003**, *47*, 2261–2267. (b) Tobin, J. G.; Moore, K. T.; Chung, B. W.; Wall, M. A.; Schwartz, A. J.; van der Laan, G.; Kutepov, A. L. *Phys. Rev. B* **2005**, *72*, 085109−11. (c) Hosono, H. *Thin Solid Films* **2007**, *515*, 6000–6014.

(28) (a) Roos, B. O.; Malmqvist, P. A.; Gagliardi, L. *J. Am. Chem. Soc.* **2006**, *128*, 17000–17006. (b) Hughes, I. D.; Däne, M.; Ernst, A.; Hergert, W.; Lüders, M.; Poulter, J.; Staunton, J. B.; Svane, A.; Szotek, Z.; Temmerman, W. M. *Nature* **2007**, *446*, 650–653.

(29) (a) Matsushita, M. M.; Kawakami, H.; Sugawara, T.; Ogata, M. *Phys. Rev. B* **2008**, *77*, 195208–6. (b) Kusamoto, T.; Kume, S.; Nishihara, H. *J. Am. Chem. Soc.* **2008**, *130*, 13844–13845.

(30) In TTF_4 model, the hydrogen-bonding part, $-COO^-NH_4^+$, was replaced by a hydrogen atom to subtract the effect of the electrostatic hydrogen-bonding interaction. Only the positions of newly-introduced hydrogen atoms were optimized with RHF/3-21G*, and single point calculation was carried out with UHF/6-31G*, assuming a radical cation ($S = 1/2$, charge = +1). C1 symmetry was adopted in this calculation.
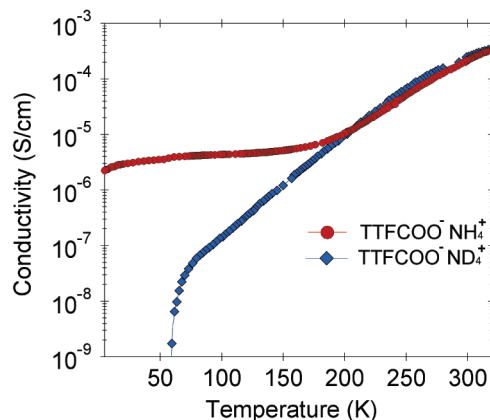
(31) Garcia-Yoldi, I.; Miller, J. S.; Novoa, J. J. *J. Phys. Chem. A,* **2009**, *113*, 484–492.

(32) (a) Catti, M.; Sandrone, G.; Dovesi, R. *Phys. Rev. B* **1997**, *55*, 16122–16131. (b) Moreira, I. P. R.; Dovesi, R.; Roetti, C.; Saunders, V. R.; Orlando, R. *Phys. Rev. B* **2000**, *62*, 7816–7823.

(33) Ivanova, A. N.; Tadjer, A. V.; Gospodinova, N. P. *J. Phys. Chem. B.* **2006**, *110*, 2555–2564.

(34) The lowered LUMO is also produced using the positively charged tetrameric model (see Figure 4b).

(35) Van de Walle, C.; Neugebauer, G. *J. Appl. Phys.* **2004**, *95*, 3851–3879.
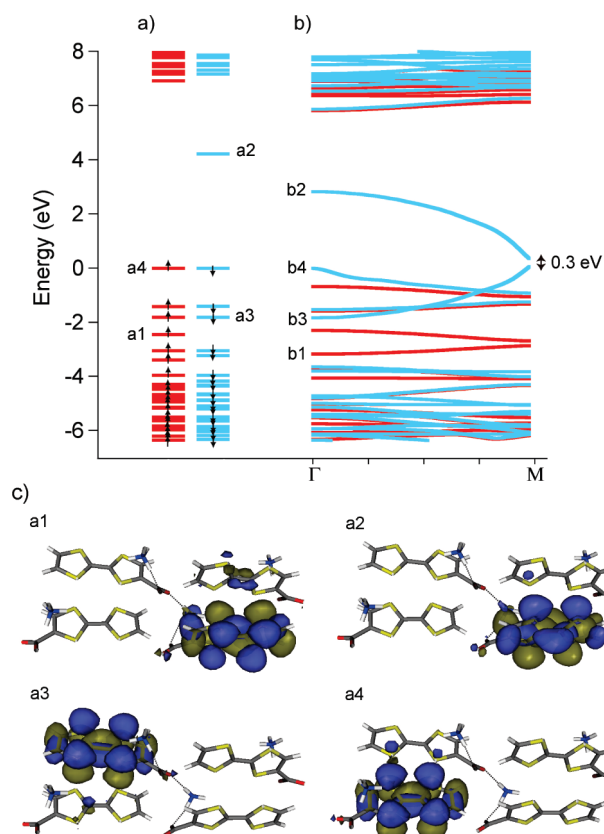
Figure 6. Electronic states of neutral tetrameric TTFCOO⁻NH₄⁺ evaluated with UHF/3-21G* adopted (a) non-PBC and (b) PBC. The highest occupied energy level is taken as origin of the energy axis. Red and blue bars represent alpha- and beta-orbitals, respectively. The inset notations mean the following: a1, SOMO; a2, LUMO; a3, beta-orbital right above SOMO; a4, HOMO; b1, PBC-SOMO; b2, PBC-LUMO; b3, split beta-orbital right above PBC-SOMO; and b4, the highest occupied energy level, respectively. (c) Molecular orbital pictures. Dotted lines represent hydrogen bonds.

with the electron conduction at M point.[36] The split orbitals are attributed to the TTF moiety, which is directly connected with TTF•⁺COO⁻NH₄⁺ by the hydrogen bonds (Figure 6c, a3). This periodic calculation strongly suggests that the embedded radical behaves as a dopant to induce the conductivity of the stacked TTF moieties assembled by the hydrogen-bonding network. Namely, TTFCOO⁻NH₄⁺ can be addressed as a "hydrogen-bonding-assisted self-doped conductor".

Ac Conductivity of the Self-Doped Hydrogen-Bonding Conductor, TTFCOO⁻NH₄⁺. Finally we show ac conductivities of TTFCOO⁻NH₄⁺, and deuterated TTFCOO⁻ND₄⁺, measured by a two-probe method at 1 MHz at temperatures ranging from 4.2 to 320 K (Figure 7). The ac conductivities for TTFCOO⁻NH₄⁺ and TTFCOO⁻ND₄⁺ at 300 K are 2.0×10^{-4} and 5.5×10^{-4} S/cm, respectively. In the temperature range from 200 to 320 K, the temperature dependence of the ac conductivities of TTFCOO⁻NH₄⁺ and TTFCOO⁻ND₄⁺ almost coincide with each other. The electronic behaviors obey the

(36) In the PBC calculation, non-degenerate alpha- and beta-orbitals are observed near the highest occupied energy level. Although the limitation of one-electron approximation of the periodic UHF method with spin-only correlation is mentioned in the calculations of transition metal oxides,[32a] particularly in this calculation, the energetic relationship between the PBC-SOMO and split alpha- and beta-orbitals strongly implies an electron-correlation effect among these three orbitals attributed to CI (so-called nondynamical electron correlation effect).[26]

Figure 7. Ac conductivities of the pelletized samples of TTFCOO⁻NH₄⁺ (red) and TTFCOO⁻ND₄⁺ (blue) measured by a two-probe method at 1 MHz from 4.2 to 320 K.

Arrhenius relation, characterizing them as activation-type transport, with activation energies of 0.16 and 0.19 eV for TTFCOO⁻NH₄⁺ and TTFCOO⁻ND₄⁺, respectively. In sharp contrast, the ac conductivities below 200 K are quite different from each other, where only TTFCOO⁻NH₄⁺ shows metallic behavior with a saturation value of 10^{-6} S/cm. Such behavior has not been observed in normal organic semiconductors with activation-type transport. On the other hand, the ac conductivity of TTFCOO⁻ND₄⁺ drops abruptly at low temperature. This behavior is similar to that of typical activation-type conductors such as proton-doped polyaniline.[37] TTFCOO⁻NH₄⁺ and TTFCOO⁻ND₄⁺ show mostly overlapping powder X-ray diffraction patterns at 300 K (Figure 8a), indicating that their crystal structures are isomorphous and their molecular arrangements are substantially identical at 300 K. In contrast, TTFCOO⁻NH₄⁺ and TTFCOO⁻ND₄⁺ show obviously different diffraction patterns at 100 K (Figure 8b). Shrinking of hydrogen bonds with decreasing temperature is a well-known phenomenon, the degree of which is generally different between species containing protons and deuterons.[38] The change of the crystal structure with shrinkage of the hydrogen-bonding network probably correlates with the different behaviors in ac conductivities between TTFCOO⁻NH₄⁺ and TTFCOO⁻ND₄⁺ at low temperature.
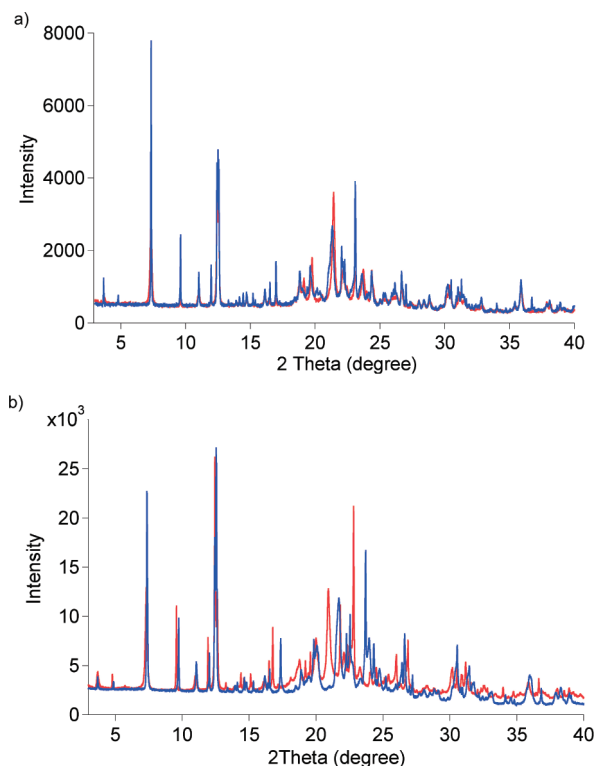
Conclusions

The present report demonstrates the radical generation triggered by the protonation of the TTF moiety, leading to conductivity in a hydrogen-bonding salt, TTFCOO⁻NH₄⁺. Spectroscopic analyses demonstrated that the spin generation in TTFCOO⁻NH₄⁺ takes place without the addition of an external dopant, which is reasonably supported by theoretical calculations. MO calculations using cluster models show that the open-shell electron contained in the hydrogen-bonding network of TTFCOO⁻NH₄⁺ is stabilized in an inert molecular orbital, being characterized as an f-electron-like electronic system with a quasi-closed-shell state. It is of great importance that such an electronic state is achieved in the absence of any metallic element. This particular open-shell state is stabilized by short S···S contacts assisted by the electrostatic hydrogen-

(37) Zuo, F.; Angelopoulos, M.; MacDiarmid, A. G.; Epstein, A. J. *Phys. Rev. B* **1989**, *39*, 3572–3577.
(38) (a) Cowan, A. J.; Howard, J. A. K.; McIntyre, G. J.; Lo, A. M.-F.; Williams, I. D. *Acta. Cryst. B* **2005**, *61*, 724–730. (b) Madsen, G. K. H.; McIntyre, G. J.; Schiøtt, B.; Larsen, F. K. *Chem.−Eur. J.* **2007**, *13*, 5539–5547.

Figure 8. Powder X-ray diffraction patterns of TTFCOO⁻NH₄⁺ (red) and TTFCOO⁻ND₄⁺ (blue) at (a) 300 K and (b) 100 K, collected from 3 to 40° (2 theta) using synchrotron radiation.

bonding interaction. The *ab initio* periodic calculation suggests that the embedded radical plays essential roles in achieving the semiconducting feature of the stacked TTF moieties. Moreover, the ac conductivity of TTFCOO⁻NH₄⁺ shows a large isotope effect at low temperature, demonstrating a strong correlation between the electronic behavior and hydrogen-bonding interaction. As far as we know, TTFCOO⁻NH₄⁺ is the first self-doped molecular conductor.

Supporting Information Available: CIF and difference plot for Rietveld refinement of crystalline TTFCOO⁻NH₄⁺. IR, ESR, ¹H NMR, ESI-TOF-MS spectra. The results of CASSCF, UMP2 calculations. Electronic states for hexameric model and TTF₄. Orbital energies and molecular orbital pictures. Complete ref 17. This material is available free of charge via the Internet at http://pubs.acs.org.

JA809425B